ADVANCED THEORY AND SIMULATIONS
www.advtheorysimul.com

Thermodynamic Modeling of the Selective Adsorption of Carbon Dioxide over Methane in the Mechanically Constrained Breathing MIL-53(Cr)

Louis Vanduyfhuys and Guillaume Maurin*

The coadsorption of CO_2/CH_4 in the breathing MIL-53(Cr) under the application of an additional mechanical pressure is investigated through the use of an extended thermodynamic mean-field model. The focus is on the breathing behavior, negative gas adsorption (NGA), and selective adsorption of CO_2 as well as to what degree the application of mechanical pressure influences this behavior. To this end, phase diagrams, coadsorption isotherms are constructed and the CO_2/CH_4 selectivity is computed in terms of the vapor pressure of methane and carbon dioxide as well as the mechanical pressure. As a result, it is found that NGA can be induced by coadsorption of CO_2/CH_4 gas mixtures with certain molar compositions. Finally, a specific adsorption/desorption cycle, which includes the application of an additional mechanical pressure, is proposed to allow for an increased CO_2/CH_4 selectivity as well as for an expected less energy demanding CO_2 desorption step.

1. Introduction

Metal-organic frameworks (MOFs) are amongst the prime candidates in the search for efficient materials for the storage/purification of natural gas as well as the capture of a series of toxic molecules.[1] The vast potential of these materials is due to their hybrid nature, consisting of metal ions or clusters interconnected by means of organic linkers, resulting in porous materials with tunable pore size and chemical functionality for the targeted adsorption/separation of the aforementioned species.[2–6] Despite their porous nature, these materials retain their long-range structural order. In this sense, they are also denoted as soft porous crystals (SPCs).[7] Furthermore, it is well known that some MOFs can undergo phase transformations induced by a wide array of triggers including adsorption of gases or liquids, mechanical pressure, temperature, electric or magnetic fields.[8,9] The resulting structural transitions, which imply large unit cell volume changes usually above 30%, are often referred to as breathing, and were originally primarily investigated when induced by adsorption.[10–13] As a result, a plethora of studies has been reported using experimental and computational approaches, that focus on the adsorption properties of breathing MOFs. Experimentally, many fascinating phenomena have been observed, from the first reports on adsorption-induced breathing of MIL-53 (MIL stands for Materials of Institute Lavoisier),[14] to multistep breathing for nitrogen in Co(bdp)[15] and the observation of negative gas adsorption (NGA) for methane in DUT-49.[16] From a computational point of view, various approaches have been proposed to investigate adsorption in breathing MOFs, ranging from force-field-based simulations[17,18] to the application of various models to determine the thermodynamic potential using either experimental or computational input.[19,20] As was mentioned before, adsorption is not the only trigger to induce structural transitions. The application of mechanical pressure has also been shown to induce similar structural transitions.[21–23] As such, by means of combined experimental and computational research, various MOFs have been proposed as possible candidates for nano dampeners or nano shock absorbers.[21–23] In most of the aforementioned studies, the focus was set on structural transitions induced by one particular trigger. However, the present authors recently proposed a generalized thermodynamic approach that was applied for the investigation of structural transitions in various MOFs induced by various triggers including temperature, mechanical pressure, and adsorption.[24] Such a generalized approach also resulted in a classification of SPCs into various types depending on their response upon application of mechanical pressure. Furthermore, the SPC type of the material was very recently linked with the adsorption-induced behavior to set up a thought experiment to explore the impact of an additional mechanical pressure on NGA.[37]

Given their fascinating adsorption properties, these breathing materials are also promising candidates to serve as efficient hosts for the separation of gas mixtures. More specifically, the separation of carbon dioxide from a given mixture is an important issue in the context of carbon capture and storage,[25] which is highly

Dr. L. Vanduyfhuys
Center for Molecular Modeling (CMM)
Ghent University
Technologiepark 46, 9052 Zwijnaarde, Belgium
E-mail: Louis.Vanduyfhuys@UGent.be
Prof. G. Maurin
Institut Charles Gerhardt Montpellier UMR 5253 CNRS UM ENSCM
Université Montpellier
Place E. Bataillon, 34095 Montpellier, Cedex 05, France

The ORCID identification number(s) for the author(s) of this article can be found under https://doi.org/10.1002/adts.201900124

DOI: 10.1002/adts.201900124

relevant in the quest for the mitigation of climate change. Another highly relevant example, is the separation of carbon dioxide from methane for an energy-efficient purification of natural gas.[26–28] Although the importance of these technologies cannot be underestimated, it is remarkable that only a few experimental studies report multicomponent adsorption isotherms particularly for breathing MOFs.[13] This can partly be rationalized by the inherently high dimensionality of the problem, leading to typically complex and time-consuming experiments. Indeed, most of the data reported on multicomponent adsorption in the literature either results from numerical or analytical models using single component isotherms obtained experimentally or simulated by grand canonical Monte Carlo simulations, or experimental breakthrough profiles.[29] Therefore, it is crucial to invest in computational techniques allowing to accurately predict the multicomponent adsorption isotherms. A common approach is the application of ideal adsorption solution theory (IAST),[30] which is relatively simple to implement. However, as indicated by Fraux et al., one has to be careful in its application for flexible adsorbents.[31] The main issue is that the basic requirements for IAST, such as an inert host material, are violated for a breathing MOF. However, Coudert et al. developed an alternative, the so-called osmotic framework adsorption solution theory (OFAST), to predict the adsorption behavior of gas mixtures in the osmotic thermodynamic ensemble starting from the pure-component and fixed-phase adsorption isotherms.[32] Maurin et al., conducted a hybrid osmotic Monte Carlo (HOMC) approach based on the use of a flexible force field to predict the coadsorption behavior of MIL-53(Cr) for diverse CO_2/CH_4 gas mixture compositions.[27] Alternatively, Dunne et al. represented the breathing MIL-53(Al) as a 1D chain, in which each bead is interpreted as a group of unit cells either in the large pore (lp) phase or narrow pore (np) phase, and applied the transfer matrix method to predict coadsorption of methane and carbon dioxide for various conditions of total vapor pressure, CH_4/CO_2 ratio and temperature. Finally, the same authors also investigated the impact of an additional mechanical pressure on the shape of the adsorption isotherms.[33]

In this work, we extend the semi-analytical mean-field model, which was originally developed for single-component adsorption in MOFs,[20] toward adsorption of binary mixtures in a breathing MOF. This model is then used for the investigation of the breathing behavior of the 1D channel like carboxylate MIL-53(Cr)[14] when exposed to a mixture of methane and carbon dioxide under varying conditions, by constructing the full phase diagram of MIL-53(Cr) as a function of the independent CH_4 and CO_2 vapor pressures. Furthermore, we explore the impact of an additional mechanical pressure on the multicomponent adsorption behavior of MIL-53(Cr) with the aim of gaining fundamental thermodynamic insight into the mechanically contraint coadsorption behavior of breathing MOFs. As such, we show that coadsorption can give rise to NGA and we demonstrate that the application of optimal conditions (mechanical pressure and gas pressure) can allow a drastic enhancement of the CO_2/CH_4 separation performance of MIL-53(Cr).

2. Methodology

In the mean-field model,[20,34] the central quantity was the Helmholtz free energy $F(N, V)$ of MIL-53(Cr) at fixed temperature ($T = 300$ K) as a function of the unit cell volume V as well as the number of adsorbed guest molecules N. In this work, the free energy was expanded in three contributions: the empty host free energy $F_{\text{host}}(V)$, the interactions between guest molecules inside the pore modeled through a van der Waals equation of state $F_{\text{vdw}}(N, V_{\text{p}}(V))$, in which $V_{\text{p}}(V)$ represents the pore volume, and the host–guest interaction $F_{\text{int}}(N, V)$ is expressed in terms of the mean-field single-particle adsorption energy $\Delta U(V)$. The most important approximations in this model are two-fold. The first consisted of using a van der Waals equation of state for the confined guests, which indeed was a reasonable approximation for analyzing qualitative behavior. The second was the mean-field approximation of the interaction energy, which ignored higher-order corrections that account for screening effects. However, for the adsorption of pure methane or carbon dioxide in MIL-53(Cr), the validity of the mean-field model in describing the qualitative behavior of breathing MOFs was already shown in previous work, as it was indeed able to reproduce the experimental observation that carbon dioxide can trigger the breathing of MIL-53(Cr), while methane cannot.[20] By performing the Legendre transform from N to μ and from V to P_{ext}, the osmotic ensemble can be accessed, which allows to compute the equilibrium unit cell volume and number of adsorbed particles as a function of chemical potential (related to the guest vapor pressure p_{vap}) and external pressure ($P_{\text{ext}} = p_{\text{vap}} + P_{\text{mech}}$). Here, the vapor pressure was denoted with small letter p and mechanical and external pressure with capital P. More details on this thermodynamic model and its approximations can be found in ref. [20]. Within the context of this work, the model had been extended toward binary adsorption. This was achieved by replacing the pure-component parameters in the van der Waals equation of state with parameters for a mixture according to mixing rules taken from ref. [35], and expressing the guest-interaction free energy with two independent mean-field interaction terms, one for each component.

$$F(N_1, N_2, V) = F_{\text{host}}(V) + F_{\text{vdw}}\big(N_1, N_2, V_{\text{p}}(V)\big) + N_1 \times \Delta U_1(V) + N_2 \times \Delta U_2(V) \quad (1)$$

As such, in addition to the limitations of the original mean-field model, this simple extension also neglects correlation terms that would account for cross screening of the interaction energy. The main focus of this investigation is to analyze the qualitative breathing behavior of MOFs induced by adsorption of binary mixtures. The Legendre transform is now again applied toward the osmotic ensemble to get access to the osmotic potential as well as the osmotic adsorption isotherm for each component of the mixture. More details on the extension of the Helmholtz free energy and the corresponding Legendre transforms can be found in Section S1, Supporting Information. The model required various input profiles: the empty host free energy profile $F_{\text{host}}(V)$, the van der Waals parameters for methane and carbon dioxide, the pore volume $V_p(V)$ figuring in the van der Waals equation of state, and the single-particle mean adsorption energy $\Delta U(V)$ for methane and carbon dioxide. The specific level of theory used to model all input required in this model was identical to the

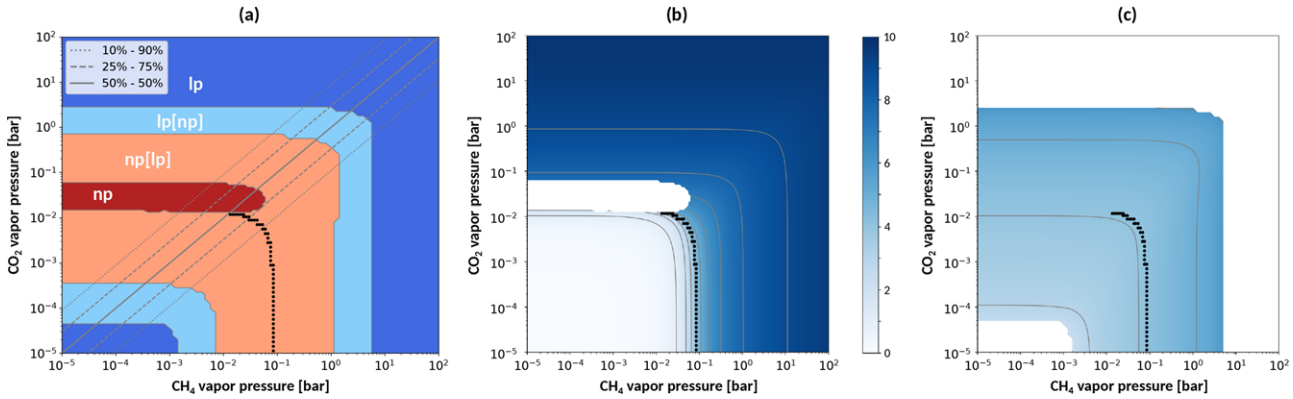

Figure 1. a) Phase diagram calculated for the coadsorption of a CO_2/CH_4 gas mixture at a temperature $T = 300$ K without an extra mechanical pressure. The system can either be in: a stable large pore (denoted by lp, indicated in dark blue), a bistable phase with a stable large pore and metastable narrow pore (denoted by lp[np], indicated in light blue), a bistable phase with a metastable large pore and stable narrow pore (denoted by np[lp], indicated in light red) or a stable narrow pore (denoted by np, indicated in dark red). b) Total number of guests adsorbed in the large pore. c) Total number of guests per unit cell adsorbed in the narrow pore. The black dots represent the contour for which the total amount per unit cell adsorbed in the large pore equals the total amount adsorbed in the narrow pore, indicating that a structural transition occurring to the right of this line will induce NGA.

original work: the empty-host free energy was fitted to experimental data on equilibrium volumes, transition pressure and bulk moduli, the van der Waals parameters were taken from experimental equations of state, the interaction energy and pore volume were computed by means of random insertion of rigid CO_2 and CH_4 molecules and computing their interaction with the framework using the Lennard-Jones model from ref. [36]. Finally, as was shown in previous work, the pore volume was represented by means of a simple piecewise linear function expressed in terms of the unit cell volume.[37]

In the remainder of this work, phase diagrams, coadsorption isotherms were constructed and the selectivity of CO_2 over CH_4 as a function of the vapor gas pressures of each component as well as the mechanical pressure was computed. To this end, the osmotic potential, equilibrium unit cell volume ,and number of adsorbed methane and carbon dioxide molecules after performing the Legendre transform expressing equilibrium with given chemical potentials μ_{CO2} and μ_{CH4} and external pressue P_{ext} were computed. It was important to be aware that such equilibrium may feature multiple solutions for the volume, number of adsorbed molecules, and osmotic potential. This was due to the inherent bistability of the system. For example, for certain conditions of the vapor pressures and mechanical pressure, two local minima were found, one with a unit cell volume in the large pore (lp) region (i.e., between 1300 and 1500 Å^3) and one with a volume in the narrow pore (np) region (between 900 and 1300 Å^3). Depending on the relative values of the corresponding osmotic potential of both solutions, the system will then either be in the phase lp(np), in which the lp solution had the lowest potential and np hence represented a metastable state, or np(lp), in which the np solution had the lowest potential and lp represented a metastable state. These phases can then be visualized in a phase diagram as a function of the applied control variables. Furthermore, the number of adsorbed methane and carbon dioxide molecules to construct the corresponding coadsorption isotherms and the resulting selectivity were computed.

3. Applications

3.1. Coadsorption of Carbon Dioxide and Methane without Mechanical Constraint

In a first stage, we consider the system in the absence of an additional mechanical pressure, in other words $P_{ext} = p_{CH4} + p_{CO2}$, and construct the phase diagram of CO_2/CH_4 mixtures adsorbed in MIL-53(Cr) as a function of the vapor pressure of both adsorbates. The results are shown in **Figure 1**. It indicates, as a function of the vapor pressure of CH_4 and CO_2, whether MIL-53(Cr) is in a monostable lp (dark blue), monostable np (dark red), bistable lp[np] (light blue), or bistable np[lp] (light red) states. Herein, lp[np] indicates that lp represents the global equilibrium, while np is a metastable state, and vice versa for np[lp].

Let us assume that we start at the lower left corner in the lp phase at very low vapor pressures, for which no molecules are adsorbed yet. Furthermore, we also assume collective behavior, in which all unit cells have to act identically and simultaneously, which in term implies that a transition from lp to np will only occur if the lp does not exist anymore as a (meta)stable state.[36] If we now consider an adsorption process, for example, a fixed equimolar CO_2/CH_4 gas mixture (molar composition of 50/50), we follow the solid gray line. As the vapor pressure of methane and carbon dioxide increases, the system changes phase from lp to lp(np) and np(lp). However, in all these phases the lp remains a (meta)stable state and in the assumption of a collective behavior, the system will remain in the lp volume state. Only when the system ends up in the np region, it will induce the transition from lp to np. From Figure 1 we can then conclude that an equimolar CO_2/CH_4 gas mixture will indeed induce the breathing of MIL-53(Cr) with increasing total vapor pressure. Moreover, given the extent of the np region on the Figure 1, we can conclude that all gas mixtures containing less than 75% methane will induce breathing. To validate the current model, we compared these predictions with previous experimental and HOMC theoretical findings for

this system. Hamon et al. applied a variety of different techniques, including in situ X-ray powder diffraction and Raman spectroscopy, to investigate the breathing behavior of MIL-53(Cr) when exposed to pure CH_4 and CO_2 as well as CO_2/CH_4 mixtures with a molar composition of 25/75%, 50/50%, and 75/25%.[27] It was found that CH_4-rich mixtures ($\geq$ 75 % CH_4) do not induce the structural transition from lp to np. This experimental evidence was supported by HOMC simulations performed in the same work. Furthermore, it was also concluded that if the structural transitions occurs, the CO_2 partial pressure at the transition is independent on the mixture composition. This is also in agreement with the current predictions, as can be seen from Figure 1 where the boundary between np[lp] (light red) and np (dark red) has a fixed value for CO_2 vapor pressure. Finally, besides this qualitative agreement with previous findings, the predicted total number of molecules required to induce the structural transition from np to lp reproduces well the data reported in ref. [27]. As such, we can conclude that the predictions resulting from the application of the current model are in excellent agreement with experimental findings. In order to estimate the sensitivity of these predictions toward the various input parameters required for the mean-field model, we performed a sensitivity analysis in which we rescaled each input with ±20%. The detailed results of this analysis can be found in the Supporting Information and indicate a rather large sensitivity. For example, making the material 20% more flexible increases the methane threshold for observing breathing from 75% to more than 90%. As such, this analysis reveals that in order to reproduce the experimental values, one requires a highly accurate free energy model.

As mentioned previously, we also want to investigate the possible occurence of NGA during the guest-induced structural transitions. Therefore, we compute the number of adsorbed methane and carbon dioxide molecules and construct the surfaces expressing the total number of adsorbed molecules in the lp (see Figure 1b) and np (see Figure 1b) forms wherever they exist as (meta)stable states. We then derive the intersection between these two surfaces, which is indicated by the black dots on the figure. If for a certain process, that is, a certain line on the phase diagram, the process line crosses the black dots before the lp-to-np transition, that is, before entering the dark red zone, NGA occurs. This is due to the fact that to the right of the black dots, the number of molecules adsorbed in the lp is larger than the number adsorbed in the np, hence upon the lp-to-np transition the number of adsorbed molecules decreases giving rise to NGA. As a result, we can derive from the figure that NGA occurs when MIL-53(Cr) is exposed to CO_2/CH_4 gas mixtures with a molar gas composition between 50/50 and 25/75. This is confirmed by constructing the coadsorption isotherm for a gas mixture with a molar gas composition of 33/66 (see top left pane of **Figure 2**). Furthermore, Figure S3, Supporting Information, which shows the coadsorption isotherm for a gas mixture with a molar gas composition of 25/75, indeed reveals no structural transition, while Figure S4, Supporting Information for a gas mixture with a molar composition of 50/50 shows a structural transition, but without NGA. In a previous study, it has been evidenced that the additional application of a mechanical pressure can be used to induce NGA in SPCs that do not exhibit adsorption-induced breathing in the absence of mechanical pressure.[37] Moreover, increasing the mechanical pressure even further subsequently induces breathing with positive gas adsorption (PGA). In other words, in terms of an increasing applied mechanical pressure, these SPCs exhibit subsequent regions of no breathing, NGA and PGA. Here, we demonstrate that coadsorption of gas mixtures with the appropriate composition of a PGA breathing-inducing gas (CO_2 in MIL-53(Cr)) with a gas that does not induce breathing (CH_4 in MIL-53(Cr))), can also induce NGA. Furthermore, by closely investigating the evolution of the number of adsorbed CH_4 (bottom left pane of Figure 2) and CO_2 (bottom right pane of Figure 2) molecules, we can conclude that NGA occurs due to a sudden expulsion of CH_4, while the amount of adsorbed CO_2 remains relatively constant. Furthermore, the top right pane shows the selectivity of CO_2 over CH_4 as a function of the vapor pressure, indicating that the selectivity can be an order of magnitude higher in the narrow pore (10-30) than in the large pore (2-6), which is consistent with the experimental findings reported by Hamon et al.[27] In other words, having a breathing transition toward a more contracted phase enhances the selective adsorption of carbon dioxide over methane, which occurs for gas mixtures with at least 25% CO_2 as mentioned before.

3.2. Impact of Mechanical Pressure on the Coadsorption of Carbon Dioxide and Methane in MIL-53(Cr)

To investigate the impact of the mechanical pressure on the coadsorption behavior of MIL-53(Cr), we consider a gas mixture with a fixed molar gas composition of 50/50 and construct the phase diagram for varying total vapor pressure $p_{tot} = p_{CH4} + p_{CO2}$ and mechanical pressure P_{mech}. The results are shown in **Figure 3**. The figure clearly illustrates that mechanical pressure has a large impact on the stability of the various phases. The black dots on the figure again represent the intersection between the surfaces of total amount adsorbed in large and narrow pore, and indicate where NGA might occur. As a result, we can derive that for the given mixture with a molar gas composition of 50/50, NGA will occur for applied mechanical pressures between −11 and 7 MPa (as indicated by the solid black lines on the figure).

As has been mentioned before, adsorption in the narrow pore is much more selective toward CO_2 than in the large pore. Furthermore, in the phase diagram of Figure 3, we notice that applying a high enough mechanical pressure ensures the system to be in the narrow pore, even for very low vapor pressures. This is due to the fact that the empty host contracts under the influence of such high mechanical pressure. The precise value at which the empty host contracts is sensitive to the way the empty host free energy profile F_{host}, which is a required input profile for the thermodynamic model, was determined. In this work, the empty host profile was taken from our previous work[36] and we found that a mechanical pressure above 105 MPa allows the contraction toward the np form. This predicted mechanical pressure is slightly above the corresponding experimental data that was evaluated for the empty MIL-53(Cr) ($\approx$ 55 MPa) framework using mercury porosimetry measurements.[38] In view of the improved selectivity in the narrow pore, we also construct the coadsorption isotherm for an equimolar gas mixture at a

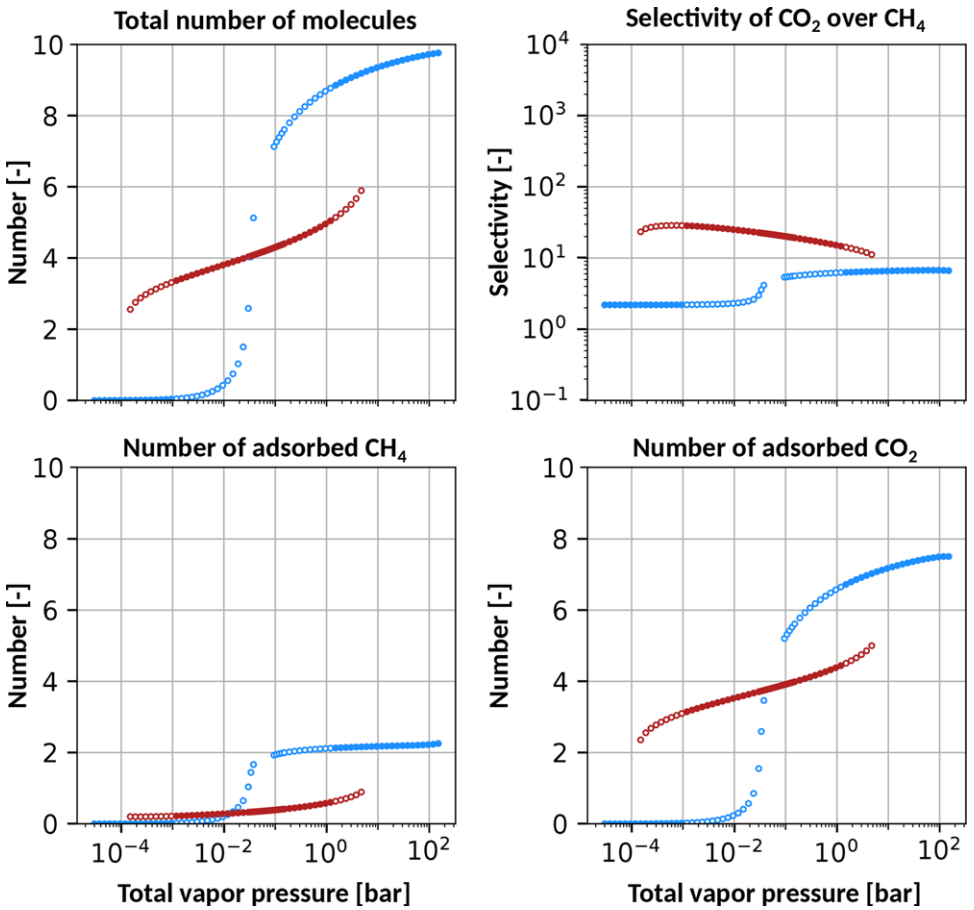

Figure 2. Coadsorption isotherms for a gas mixture with a molar gas composition of 33/66 (CO_2/CH_4) at $T = 300$ K and without the application of a mechanical pressure. The color code is as follows: full blue dots indicate a globally stable large pore state, blue circles indicate a metastable large pore, full red dots indicate a globally stable narrow pore, and red circles indicate a metastable narrow pore. The numbers of gas molecules reported in these figures are per unit cell.

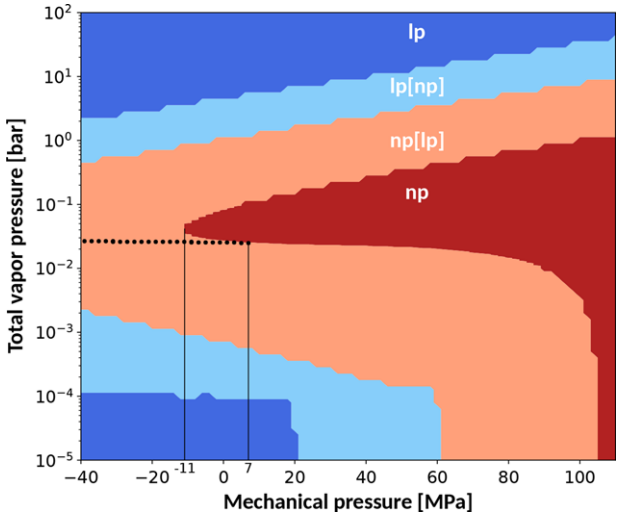

Figure 3. Phase diagram for the coadsorption of a CO_2/CH_4 gas mixture with a molar gas composition of 50/50 at varying mechanical pressure and a temperature $T = 300$ K. The solid black lines indicate the mechanical pressure range where breathing with NGA occurs.

mechanical pressure of 110 MPa, which is slightly above the contraction threshold of the empty framework of 105 MPa. The results are shown in **Figure 4**. From this figure, we can deduce that due to the application of the mechanical pressure, the system starts in the narrow pore at very low vapor pressure. As a result, as soon as saturation is reached upon increasing the total vapor pressure, the system will operate at conditions with the increased selectivity of the narrow pore. More specifically, due to the mechanical pressure, the higher selectivity is already obtained for very low vapour pressures, that is, $p_{tot} = 10^{-4}$ bar, which is much lower than in the case without mechanical pressure, where gas adsorption itself needs to induce the transition at vapor pressures of approximately $p_{tot} = 5 \times 10^{-2}$ bar (see Figure S4, Supporting Information).

In **Figure 5** we investigate the impact of increasing the mechanical pressure even further. From the figure we can conclude that upon increasing the mechanical pressure, the selectivity increases up to 100 for $P_{mech} = 400$ MPa. Furthermore, we observe that such higher selectivity can be maintained for larger vapor pressures as well. This can be understood by investigating the unit cell volume (upper left pane of Figure 5), which reveals that the high mechanical pressure forces MIL-53(Cr) to be in a narrow

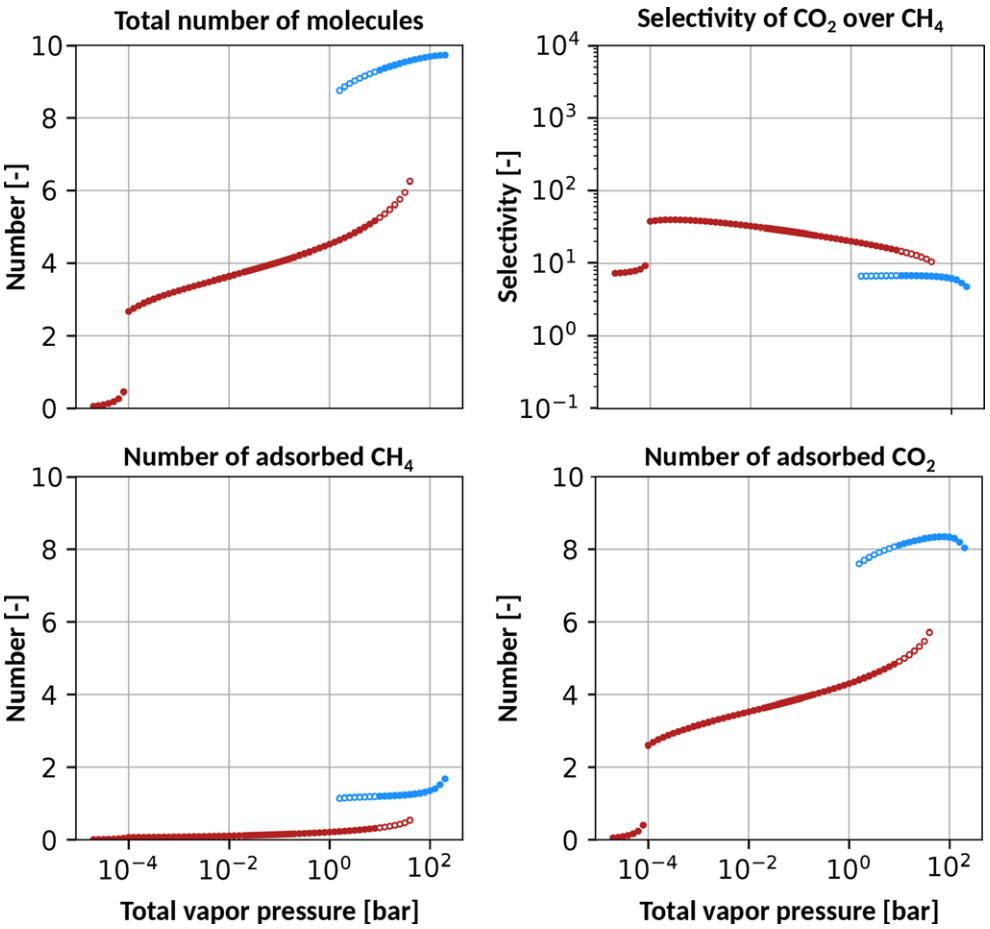

Figure 4. Coadsorption isotherms for a CO_2/CH_4 with a molar composition of 50/50 at temperature $T = 300$ K and an applied mechanical pressure of 110 MPa. The color code is as follows: full blue dots indicate a globally stable large pore state, blue circles indicate a metastable large pore, full red dots indicate a globally stable narrow pore, and red circles indicate a metastable narrow pore.

pore with unit cell volumes even lower (down to 1000 Å^3) than in the absence of mechanical pressure and hence results in the high selectivity. Even though this in turn decreases the methane uptake to values very close to zero, the uptake never reaches zero exactly. This explains why the selectivity becomes very high (up to 100), but not infinite. The underlying reasons are the entropic terms $k_BT \times \ln N_1! + k_BT \times \ln N_2!$ present in the van der Waals free energy contribution arising from the distinguishability of methane and carbon dioxide (see Equation (1.9), Supporting Information). These terms prohibit the number of methane molecules to ever reach zero, explaining why the model does not predict a perfect molecular sieving effect. Finally, we also observe that the vapor pressure upon which the narrow pore is saturated with CO_2 decreases with increasing mechanical pressure, reaching values around 2×10^{-5} bar for $P_{mech} = 400$ MPa. This could be used to design a specific adsorption cycle with an additional mechanical pressure that would allow the use of a lower heating temperature to desorb CO_2 from the open pore, which in turn implies weaker interactions with CO_2 compared to the narrow pore. The cycle would consist of the following steps: 1) applying a mechanical pressure high enough to make the empty material switch towards the empty narrow pore, 2) exposing the resulting narrow pore to CO_2/CH_4 mixtures of equimolar composition with a vapor pressure at saturation allowing for selective adsorption of CO_2, 3) releasing the mechanical pressure to reopen the material to the lp and finally 4) desorbing the adsorbed CO_2 from the lp by decreasing the vapor pressure. The suggested cycle is based on some important conditions. The applied mechanical pressure should be high enough to ensure not only the transition of the empty framework to the narrow pore, but also that the vapor pressure required for saturation of the narrow pore is lower than the upper limit of the lp region as indicated in the phase diagram of Figure 3, which is around 10^{-4} bar. In this way, releasing the mechanical pressure from the saturated narrow pore will reopen the host to its large pore version. Finally, by desorbing the carbon dioxide from the open pore, the heat required for desorption decreases drastically since CO_2 interacts much less strongly with MIL-53(Cr) in its open pore compared to its narrow pore owing to a lower degree of confinement. As such, the proposed cycle is expected to favor a highly selective adsorption of carbon dioxide over methane with a lower energy demanding regeneration process.

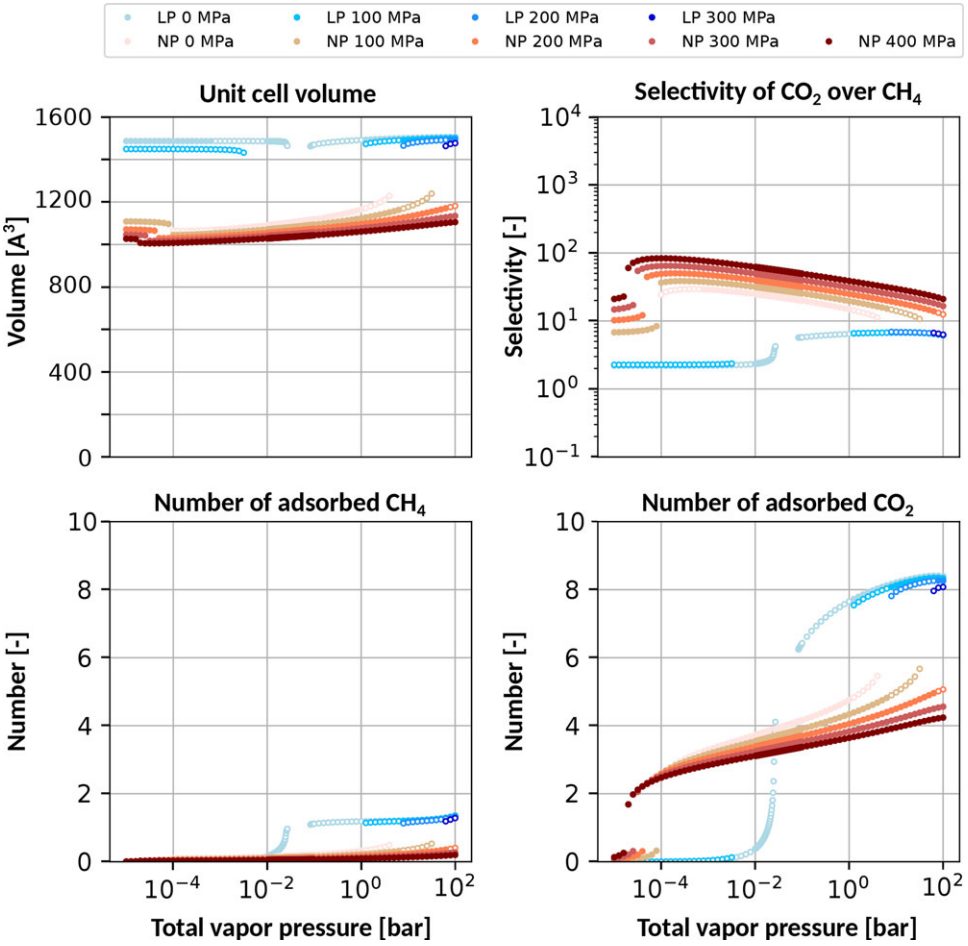

Figure 5. Coadsorption isotherms for a CO_2/CH_4 with a molar composition of 50/50 at temperature $T = 300$ K and varying mechanical pressure.

4. Conclusion

The mean-field thermodynamic model for adsorption of guest molecules in nanoporous materials has been extended toward binary adsorption and applied to co-adsorption of methane and carbon dioxide in MIL-53(Cr). By deriving the equilibrium unit cell volume of MIL-53(Cr) and computing the corresponding thermodynamic potential in the osmotic ensemble at fixed conditions of chemical potential (or vapor pressure) and mechanical pressure, a phase diagram was constructed as a function of the vapor pressure of methane and carbon dioxide. As such, it was found that CH_4-rich mixtures (molar composition > 75 %) do not induce a structural transition in MIL-53(Cr), consistent with previous experimental findings and hence validating the accuracy of the applied model. Moreover, it was also predicted that for mixtures with a fraction of methane between 50 % and 75 %, the initial structural transition from lp to np was accompanied by NGA, which has not been observed yet to the best of our knowledge. Furthermore, the impact of applying additional mechanical pressure was investigated. It was found that for a 50/50 mixture, NGA is observed for mechanical pressures between −11 and 7 MPa. Finally, the application of a mechanical pressure high enough on the empty MOF ensures that we start with MIL-53(Cr) in the narrow pore which implies that upon subsequently increasing the vapor pressure the MOF will start to selectively adsorb CO_2 over CH_4 as soon as saturation occurs for the narrow pore. This is in contrast with the situation without mechanical pressure, since selective adsorption will then only start upon the adsorption-induced transition toward the narrow pore, which occurs at higher vapor pressures. Furthermore, we have shown that mechanical pressure can also be used to design a process that allows for selective adsorption with an easier regeneration. As such, we have shown that the application of mechanical pressure can be used to tune the coadsorption behavior of mixtures in breathing MOFs, specifically with respect to the occurence of NGA and gas separation. A more systematic computational exploration of diverse mechanical-constrained separations in a series of flexible and breathing MOFs is ongoing, for example, the typical case of propane/propylene kinetic separation in ZIF-8.[39] This will be further validated in the future with the development of a lab prototype that will allow the exploration of the separation processes under mechanical constraint.

Acknowledegments

This work is supported by the Fund for Scientific Research Flanders (FWO), and the ANR Project MeaCoPA (ANR- 17-CE29-0003). The computational resources (Stevin Supercomputer

Infrastructure) and services used in this work were provided by the VSC (Flemish Supercomputer Center), funded by Ghent University, FWO and the Flemish Government—department EWI.

Supporting Information

Supporting Information is available from the Wiley Online Library or from the author.

Conflict of Interest

The authors declare no conflict of interest.

Keywords

CO_2/CH_4 selectivity, mechanical pressure, metal-organic framework, multicomponent adsorption, negative gas adsorption, regeneration, thermodynamic model

Received: June 25, 2019
Revised: July 31, 2019
Published online:

[1] H. Li, K. Wang, Y. Sun, C. T. Lollar, J. Li, H. C. Zhou, *Mater. Today* **2018**, *21*, 108.
[2] H. Furukawa, K. E. Cordova, M. O'Keeffe, O. M. Yaghi, *Science* **2013**, *341*, 1230444.
[3] A. J. Howarth, Y. Liu, P. Li, Z. Li, T. C. Wang, J. T. Hupp, O. K. Farha, *Nat. Rev. Mater.* **2015**, *1*, 15018.
[4] S. M. J. Rogge, A. Bavykina, J. Hajek, H. Garcia, A. I. Olivos-Suarez, A. Sepúlveda-Escribano, A. Vimont, G. Clet, P. Bazin, F. Kapteijn, M. Daturi, E. V. Ramos-Fernandez, F. X. Llabrés i Xamena, V. Van Speybroeck, J. Gascon, *Chem. Soc. Rev.* **2017**, *46*, 3134.
[5] K. Adil, Y. Belmabkhout, R. S. Pillai, A. Cadiau, P. M. Bhatt, A. H. Assen, G. Maurin, *Chem. Soc. Rev.* **2017**, *46*, 3402.
[6] G. Maurin, C. Serre, A. Cooper, G. Férey, *Chem. Soc. Rev.* **2017**, *46*, 3104.
[7] S. Horike, S. Shimomura, S. Kitagawa, *Nat. Chem.* **2009**, *1*, 695.
[8] A. Schneemann, V. Bon, I. Schwedler, I. Senkovska, S. Kaskel, R. A. Fischer, *Chem. Soc. Rev.* **2014**, *43*, 6062.
[9] A. Ghoufi, K. Benhamed, L. Boukli-Hacene, G. Maurin, *ACS Centr. Sci.* **2017**, *3*, 394.
[10] S. Kitagawa, R. Kitaura, S. I. Noro, *Angew. Chem. Int. Ed.* **2004**, *43*, 2334.
[11] C. Serre, S. Bourrelly, A. Vimont, N. Ramsahye, G. Maurin, P. Llewellyn, M. Daturi, Y. Filinchuk, O. Leynaud, P. Barnes, G. Férey, *Adv. Mater.* **2007**, *19*, 2246.
[12] G. Férey, C. Serre, *Chem. Soc. Rev.* **2009**, *38*, 1380.
[13] G. Férey, C. Serre, T. Devic, G. Maurin, H. Jobic, P. L. Llewellyn, G. De Weireld, A. Vimont, M. Daturi, J. S. Chang, *Chem. Soc. Rev.* **2011**, *40*, 550.
[14] C. Serre, F. Millange, C. Thouvenot, M. Noguès, G. Marsolier, D. A. Louër, G. Férey, *J. Am. Chem. Soc.* **2002**, *124*, 13519.
[15] F. Salles, G. Maurin, C. Serre, P. L. Llewellyn, C. Knöfel, H. J. Choi, Y. Filinchuk, L. Oliviero, A. Vimont, J. R. Long, G. Férey, *J. Am. Chem. Soc.* **2010**, *132*, 13782.
[16] S. Krause, V. Bon, I. Senkovska, U. Stoeck, D. Wallacher, D. M. Többens, S. Zander, R. S. Pillai, G. Maurin, F. X. Coudert, S. Kaskel, *Nature* **2016**, *532*, 348.
[17] F. Salles, A. Ghoufi, G. Maurin, R. G. Bell, C. Mellot-Draznieks, G. Férey, *Angew. Chem. Int. Ed.* **2008**, *47*, 8487.
[18] S. M. J. Rogge, R. Goeminne, R. Demuynck, J. J. Gutiérrez-Sevillano, S. Vandenbrande, L. Vanduyfhuys, M. Waroquier, T. Verstraelen, V. Van Speybroeck, *Adv. Theory Simulat.* **2019**, *2*, 1800177.
[19] F. X. Coudert, M. Jeffroy, A. H. Fuchs, A. Boutin, C. Mellot-Draznieks, *J. Am. Chem. Soc.* **2008**, *130*, 14294.
[20] L. Vanduyfhuys, A. Ghysels, S. Rogge, R. Demuynck, V. Van Speybroeck, *Mol. Simulat.* **2015**, *41*, 1311.
[21] P. G. Yot, Z. Boudene, J. Macia, D. Granier, L. Vanduyfhuys, T. Verstraelen, V. Van Speybroeck, T. Devic, C. Serre, G. Férey, N. Stock, G. Maurin, *Chem. Commun.* **2014**, *50*, 9462.
[22] P. G. Yot, L. Vanduyfhuys, E. Alvarez, J. Rodriguez, J. P. Itié, P. Fabry, N. Guillou, T. Devic, I. Beurroies, P. L. Llewellyn, V. Van Speybroeck, C. Serre, G. Maurin, *Chem. Sci.* **2016**, *7*, 446.
[23] P. Ramaswamy, J. Wieme, E. Alvarez, L. Vanduyfhuys, J. P. Itié, P. Fabry, V. Van Speybroeck, C. Serre, P. G. Yot, G. Maurin, *J. Mater. Chem. A* **2017**, *5*, 11047.
[24] L. Vanduyfhuys, S. Rogge, J. Wieme, S. Vandenbrande, G. Maurin, M. Waroquier, V. Van Speybroeck, *Nat. Comm.* **2018**, *9*, 204.
[25] J. M. Huck, L. C. Lin, A. H. Berger, M. N. Shahrak, R. L. Martin, A. S. Bhown, M. Haranczyk, K. Reuter, B. Smit, *Energy Environ. Sci.* **2014**, *7*, 4132.
[26] V. Finsy, L. Ma, L. Alaerts, D. D. Vos, G. Baron, J. Denayer, *Micropor. Mesopor. Mat.* **2009**, *120*, 221.
[27] L. Hamon, P. L. Llewellyn, T. Devic, A. Ghoufi, G. Clet, V. Guillerm, G. D. Pirngruber, G. Maurin, C. Serre, G. Driver, W. van Beek, E. Jolimaître, A. Vimont, M. Daturi, G. Férey, *J. Am. Chem. Soc.* **2009**, *131*, 17490.
[28] N. K. Jensen, T. E. Rufford, G. Watson, D. K. Zhang, K. I. Chan, E. F. May, *J. Chem. Eng. Data* **2012**, *57*, 106.
[29] J. R. Li, Y. Ma, M. C. McCarthy, J. Sculley, J. Yu, H. K. Jeong, P. B. Balbuena, H. C. Zhou, *Coordin. Chem. Rev.* **2011**, *255*, 1791.
[30] A. L. Myers, J. M. Prausnitz, *AIChE J.* **1965**, *11*, 121.
[31] G. Fraux, A. Boutin, A. H. Fuchs, F. X. Coudert, *Adsorption* **2018**, *24*, 233.
[32] F. X. Coudert, *Phys. Chem. Chem. Phys* **2010**, *12*, 10904.
[33] L. J. Dunne, G. Manos, *Philos. T. Roy. Soc. A* **2018**, *376*, 20170151.
[34] D. Bousquet, F. X. Coudert, A. Boutin, *J. Chem. Phys.* **2012**, *137*, 044118.
[35] T. Kwak, G. Mansoori, *Chem. Eng. Science* **1986**, *41*, 1303.
[36] A. Ghysels, L. Vanduyfhuys, M. Vandichel, M. Waroquier, V. Van Speybroeck, B. Smit, *J. Phys. Chem. C* **2013**, *117*, 11540.
[37] L. Vanduyfhuys, V. Van Speybroeck, *Commun. Phys.* **2019**, https://doi.org/10.1038/s42005-019-0204-y.
[38] P. G. Yot, Q. Ma, J. Haines, Q. Yang, A. Ghoufi, T. Devic, C. Serre, V. Dmitriev, G. Férey, C. Zhong, G. Maurin, *Chem. Sci.* **2012**, *3*, 1100.
[39] B. Zheng, G. Maurin, *Angew. Chem. Int. Ed.* **2019**. https://doi.org/10.1002/anie.201906245.

